JOURNAL OF VIROLOGY, Oct. 2009, p. 10417–10426 Vol. 83, No. 20
0022-538X/09/$08.00+0 doi:10.1128/JVI.00514-09

Host Genetic Variation Affects Resistance to Infection with a Highly Pathogenic H5N1 Influenza A Virus in Mice▽†

Adrianus C. M. Boon,[1] Jennifer deBeauchamp,[1] Anna Hollmann,[1] Jennifer Luke,[1] Malak Kotb,[3] Sarah Rowe,[3] David Finkelstein,[2] Geoffrey Neale,[2] Lu Lu,[4] Robert W. Williams,[4] and Richard J. Webby[1]*

Department of Infectious Diseases, St. Jude Children's Research Hospital, Memphis, Tennessee 38105[1]; Hartwell Center for Biotechnology and Bioinformatics, St. Jude Children's Research Hospital, Memphis, Tennessee 38105[2]; VA Medical Center and MidSouth Center for Biodefense and Security, Memphis, Tennessee 38104[3]; and Department of Anatomy and Neurobiology, University of Tennessee Health Science Center, Memphis, Tennessee 38105[4]

Received 12 March 2009/Accepted 21 July 2009

Despite the prevalence of H5N1 influenza viruses in global avian populations, comparatively few cases have been diagnosed in humans. Although viral factors almost certainly play a role in limiting human infection and disease, host genetics most likely contribute substantially. To model host factors in the context of influenza virus infection, we determined the lethal dose of a highly pathogenic H5N1 virus (A/Hong Kong/213/03) in C57BL/6J and DBA/2J mice and identified genetic elements associated with survival after infection. The lethal dose in these hosts varied by 4 logs and was associated with differences in replication kinetics and increased production of proinflammatory cytokines CCL2 and tumor necrosis factor alpha in susceptible DBA/2J mice. Gene mapping with recombinant inbred BXD strains revealed five loci or *Qivr* (*q*uantitative trait loci for *i*nfluenza *v*irus *r*esistance) located on chromosomes 2, 7, 11, 15, and 17 associated with resistance to H5N1 virus. In conjunction with gene expression profiling, we identified a number of candidate susceptibility genes. One of the validated genes, the hemolytic complement gene, affected virus titer 7 days after infection. We conclude that H5N1 influenza virus-induced pathology is affected by a complex and multigenic host component.

The last 10 years have witnessed a spread of highly pathogenic H5N1 avian influenza A virus from Southeast Asia into Europe and Africa, killing millions of chickens and ducks. Mammalian species including tigers, cats, dogs, and humans have also been infected with H5N1 virus, causing severe and often fatal disease. Excess mortality in humans was associated with high pharyngeal viral loads and increased cytokine and chemokine production (12). Some evidence suggests that genetic variation among infected hosts contributes to H5N1 infection and pathogenesis. Compared to the many millions of chickens and ducks that have been infected by H5N1 virus, relatively few humans have been infected. Were these individuals genetically predisposed, and therefore, did they have a greater risk of getting infected by the currently circulating H5N1 influenza viruses? Also, among the identified clusters of human H5N1 virus infections, more than 90% of the cases have occurred in genetically related family members, suggesting a possible genetic susceptibility to infection or severe disease (33). Recently, genetic relatedness was shown to be a significant risk factor for severe disease resulting from H3N2 influenza virus infection (2). However, other recent studies either have been unable to confirm the effect of genetic variation on the outcome and severity of influenza A virus infection (19) or have challenged the role of host genetics in H5N1 virus clusters (36).

Genetic polymorphisms in the infected host affect microbial pathogenesis. In some host-pathogen studies, individual genes strongly regulated disease susceptibility or severity. For example, a 32-amino-acid deletion in the *CCR5* product has been associated with increased resistance to human immunodeficiency virus infection (26), and more recently, a single amino acid change in the *TLR3* product was associated with herpes simplex virus-induced encephalitis (50). Despite these examples, most host-pathogen interactions are more complex and modified by several genetic determinants. In the mouse model, disease severity after infection with viruses, bacteria, or parasites is frequently caused by multiple genetic differences, each affecting the outcome of the disease (3, 7, 8, 17, 47). Genetic modifiers that are associated with increased susceptibility to influenza virus infection or disease are mostly unknown. In humans, the duration of virus shedding was reduced in HLA-$A2^+$ individuals, possibly as a result of a stronger cellular immune response (9). In mice, the resistance to influenza virus infection was mapped to the MX1 protein (39, 44, 46). The human MX1 protein also restricts viral replication, but its efficacy depends on the virus strain (13).

Although much work is being done to define the viral factors affecting H5N1 influenza virus pathogenesis, little has been done to elucidate the effect of host genetics on H5N1 disease outcome. This study was initiated to assess the effect of the host's genetic variation on H5N1 influenza virus pathogenesis and to provide the first clues about which host genes are responsible for the increased pathogenesis of H5N1 virus in-

* Corresponding author. Mailing address: St. Jude Children's Research Hospital, Department of Infectious Diseases, Mailstop 330, 262 Danny Thomas Place, Memphis, TN 38105. Phone: (901) 495-3014. Fax: (901) 523-2622. E-mail: Richard.Webby@stjude.org.

† Supplemental material for this article may be found at http://jvi.asm.org/.

▽ Published ahead of print on 12 August 2009.

fection. Genome-wide linkage analysis using BXD recombinant inbred (BXD RI) strains was performed to identify areas on the chromosome that contribute to the difference in susceptibility to H5N1 virus seen between C57BL/6J and DBA/2J mice.

MATERIALS AND METHODS

Animals and viruses. Six- to 11-week-old female DBA/2J (D2), C57BL/6J (B6), B10.D2.Hc^1 (B10.D2-Hc^1 H2d H2-T18c/nSnJ), and B10.D2.Hc^0 (B10.D2-Hc^0 H2d H2-T18c/oSnJ) mice were purchased from the Jackson Laboratory (Bar Harbor, ME) and housed at St. Jude Children's Research Hospital according to the institution's Animal Care and Use Committee guidelines. BXD RI mouse lines were derived from crosses between B6 and D2 mice and were acquired from three different sources. BXD1-42 mice, originally generated by Taylor et al. in the early 1980s and 1990s (42), were purchased from the Jackson Laboratory. BXD43-100 mice were obtained from the University of Tennessee Health Science Center (Memphis, TN) or purchased from the Oak Ridge National Laboratory (ORNL; Oak Ridge, TN) (35). All mice were female and between 6 and 12 weeks of age. The genomes of the mouse strains do not encode a functional Mx1 protein. All studies have been approved by the St. Jude Children's Research Hospital Institutional Review Board.

A highly pathogenic H5N1 influenza A virus was rescued by reverse genetics as described previously (21). The virus contains seven gene segments of A/Hong Kong/213/2003 H5N1 virus and the PB1 gene segment from A/Chicken/Hong Kong/Y0562/2002 H5N1 virus. This highly pathogenic H5N1 virus, referred to as HK213, was selected for its reduced lethality in B6 and BALB/c mice compared to that of wild-type A/Hong Kong/213/2003 virus (data not shown), while retaining its lethality in D2 mice, increasing the range of our phenotypic screen.

Influenza A virus infection of mice. Mice were sedated with 2,2,2-tribromoethanol (Avertin; Sigma-Aldrich, St. Louis, MO) and inoculated intranasally with highly pathogenic avian H5N1 influenza A virus. The 50% mouse lethal dose (MLD_{50}) was determined after infection with 10-fold serial dilutions of HK213 virus starting at 10^6 50% egg infective doses (EID_{50}) in 30 μl phosphate-buffered saline (PBS). Morbidity, which was measured by weight loss on days 4, 7, 10, 13, and 15 after inoculation, and mortality were monitored, and the MLD_{50} for each mouse strain was calculated using the Reed-Muench method (38). LD_{50} assays were done a least twice, and a minimum of five mice per dose of H5N1 virus were used per assay. For survival times and mortality rates, we used death as an end point. All mice included in this study were productively infected with influenza A virus as determined by lung viral titers or a significant decrease (>5%) in weight on day 4 or 7.

BXD RI strains were inoculated with an intermediate dose (10^4 EID_{50}) of HK213 virus in 30 μl PBS, and morbidity and mortality were monitored for 30 days. Survival time (measured in days) and mortality rate (percentage of mice that succumbed to infection) were calculated for each BXD RI strain.

Lung viral titers and immunohistochemistry. HK213 virus-infected lungs were harvested on days 2, 4, and 7 after infection and stored at −80°C. Lungs were then homogenized in 2.0-ml tubes containing 1.0 ml minimum essential medium and a stainless steel ball for two 30-s periods at maximum frequency (30 Hz; TissueLyzer; Qiagen). The homogenate was spun for 5 min at 1,000 × *g* to remove cellular debris. The virus-containing supernatant was then titrated on MDCK cells as previously described (38).

Immunohistochemistry was performed on formalin-fixed lung tissue harvested from HK213 virus-infected or uninfected D2 mice and B6 mice. Following antigen retrieval using an EDTA buffer (pH 8.0; Zymed Laboratories Inc., South San Francisco, CA), influenza virus was detected with a polyclonal goat anti-influenza A virus antibody (United States Biological, Swampscott, MA) followed by a secondary donkey anti-goat antibody conjugated to biotin (Santa Cruz Biotechnology, Santa Cruz, CA) and streptavidin-horseradish peroxidase. Viral protein was visualized using 3,3′-diaminobenzidine, and slides were counterstained with hematoxylin.

Cytokine analysis. Lungs from B6, D2, BXD43, BXD68, BXD73, BXD67, and BXD97 mice infected with 10^4 EID_{50} were obtained 3 days after infection and immediately homogenized in 2.0-ml tubes containing 1.0 ml PBS and a stainless steel ball for two 30-s periods at 30 Hz (TissueLyzer). After a 30-s spin at 16,000 × *g*, the supernatant was collected, aliquoted, and stored at −80°C. The amounts of chemokine (C-C motif) ligand 2 (CCL2) and tumor necrosis factor alpha (TNF-α) present in the lung homogenates of infected animals were determined using Quantikine kits from R&D Systems (Minneapolis, MN). The concentrations of alpha and beta interferon (IFN-α and -β, respectively) present in the homogenate were determined with the IFN-α or -β kit from PBL Laboratories (Piscataway, NJ). The average values represent data from three to six mice per strain. This analysis was repeated in BXD73, D2, and B6 mice.

QTL mapping. Mapping of quantitative trait loci (QTL) was performed using the WebQTL module of GeneNetwork (www.genenetwork.org). Interval mapping evaluates potential QTL at regular intervals and estimates the significance at each location by using 1,000 permutation tests (11, 35). Mapping was done with 66 different BXD RI strains for survival time (measured in days) after infection with highly pathogenic H5N1 virus and for mortality rate. For the original data set, see www.genenetwork.org (identification numbers 10865 and 10866). Five different loci associated with survival after infection were identified and will be referred to as *Qivr* (*Q*TL for *i*nfluenza *v*irus *r*esistance). For example, *Qivr2* is the first identified locus on chromosome 2 that is significantly associated with survival after H5N1 influenza virus infection. Linkage analysis using genetic markers located centrally in each of the five loci identified a significant linkage for *Qivr15* with *Qivr7* and *Qivr11* (Spearman $R^2 > 0.5$ and $P < 0.05$; data not shown). Pair-scan and composite analysis demonstrated that the *Qivr* act mostly independently and the effects of each *Qivr* add to the H5N1 resistance phenotype. Effect size of individual loci was determined by univariate analysis of variance (ANOVA).

RNA isolation and functional genomics. RNA expression was analyzed in lungs from either uninfected or HK213 virus-infected (10^4 EID_{50}) D2 mice and B6 mice and also in HK213 virus-infected (10^4 EID_{50}) resistant (BXD43, BXD68, and BXD98) and susceptible (BXD67, BXD83, BXD73 and BXD97) BXD mice. A minimum of three RNA samples per strain or treatment group was obtained. Following homogenization of the tissue in TRIzol (Sigma), RNA was extracted and submitted to a cleanup protocol (Qiagen).

RNA quality was confirmed by UV spectrophotometry and by analysis on an Agilent 2100 bioanalyzer (Agilent Technologies, Santa Clara, CA). Total RNA (5 to 10 μg) was processed in the St. Jude Hartwell Center for Biotechnology & Bioinformatics by using the Affymetrix eukaryote one-cycle target-labeling protocol (http://www.affymetrix.com/support/technical/manual/expression_manual.affx). Expression analyses were performed on RNA samples from individual mice using the Affymetrix Mouse MOE-430v2 GeneChip array, which interrogates more than 39,000 transcripts. Signal values and detection calls were generated using the default parameters within the statistical algorithm of the Affymetrix GCOS software version 1.4. Signal values were scaled to a 2% trimmed mean target value of 500. Probe set annotations were obtained from the Affymetrix website (http://www.affymetrix.com/analysis/index.affx).

Statistical analysis. Statistical analysis of differences in survival after H5N1 virus infection was performed by a log-rank test, and *P* values of <0.01 were considered significant. A Student *t* test was used to analyze the differences in lung virus titers between the different strains of mice following natural log (ln) transformation of the data. Chemokine and cytokine production was analyzed by *t* test, and *P* values of less than 0.05 were considered significant.

Data from Affymetrix mouse 430v2 whole-genome arrays were summarized by the MAS5.0 algorithm. The signal values were then ln-start transformed, ln(signal + 20), to stabilize variance across the range of intensity and approximate normality in preparation for parametric tests. Using Partek Genomics Suite 6.3, we applied a two-factor ANOVA model with an interaction term to the transformed signal data for each probe set on the arrays. The two model factors were mouse breed and infection status and were treated as categorical variables in the model. The interaction term was a test of whether a change in expression due to infection was influenced by breed to a degree greater than that expected by chance. The resulting full-model *P* values were adjusted using the false-discovery rate method (6). Setting the acceptable false-discovery rate to 1%, we determined that 4,447 probe sets had significant changes in expression. The *P* values for each model term, as well as for the interaction, were captured. By comparing the partial *P* values for each probe set, we assessed which factor best explains the expression pattern of a given transcript.

Log base-2 ratios were calculated from the log2-transformed ratio of the geometric means of the MAS5.0 signal data adjusted by the small additive factor of 20. The addition of 20 to the MAS5.0 signal affects a soft threshold on the data, whereby the influence of very small numbers on the log ratios is attenuated. Change is determined by expressing the absolute value of the log ratios as a power of 2, i.e., a log ratio of 3 is 2^3 or eightfold changed. For log ratios of less than 1, the change is noted as negative.

RESULTS

Differences in susceptibility to highly pathogenic H5N1 influenza A virus in two inbred strains of mice. To quantify the effect of host genetics on H5N1 disease susceptibility, we in-

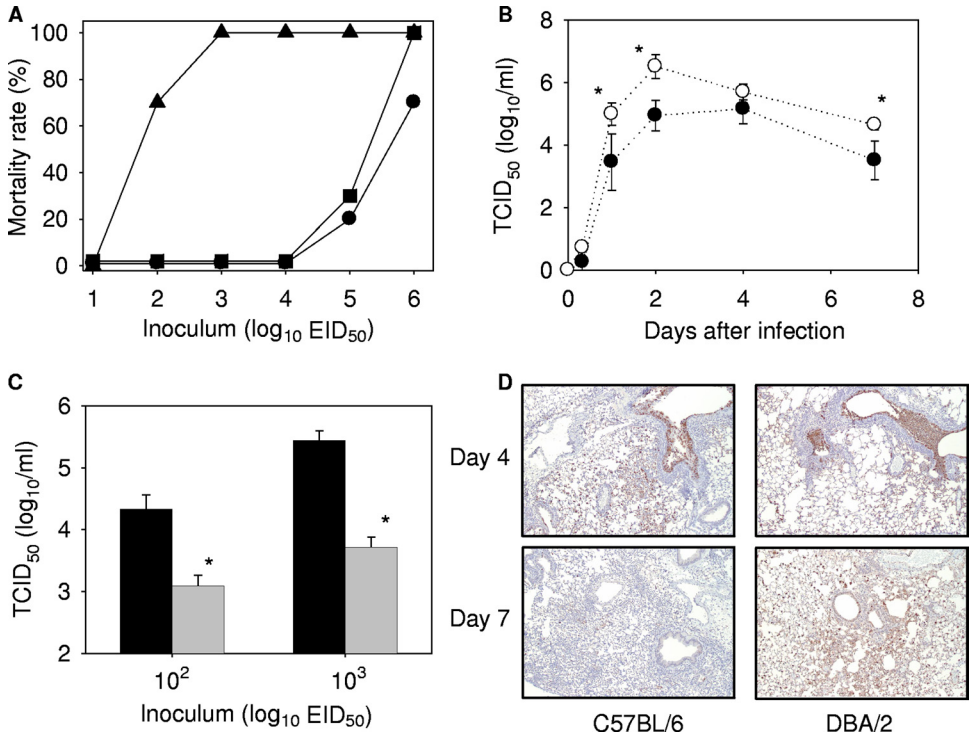

FIG. 1. Increased susceptibility to H5N1 virus infection of DBA/2J (D2) mice. (A) D2 mice (triangles), B6 mice (circles), and B6D2F1 mice (squares) were inoculated with a 10-fold serial dilution of HK213 H5N1 virus in 30 μl PBS ($n = 5$ mice per dilution). The mortality rate was monitored for 30 days, and the average mortality from two independent experiments is presented. (B) B6 mice (filled circles) and D2 mice (open circles) were inoculated with 10^4 EID_{50} of HK213 virus in 30 μl PBS. The lungs were isolated at multiple time points after infection, and the virus titer was determined. The average virus titer ± standard deviation ($\log_{10}$ 50% tissue culture infective doses [$TCID_{50}$]/ml) at 8 and 24 h postinfection represents one experiment with five mice per group; the average virus titers on days 2, 4, and 7 postinfection represent multiple experiments with at least four mice per group. *, $P < 0.001$. (C) B6 mice (gray bars) and D2 mice (black bars) were inoculated with 10^2 or 10^3 EID_{50} of HK213 virus in 30 μl PBS. Forty-eight hours later, the lungs were isolated, and the virus titer was determined. *, $P < 0.001$. (D) Immunohistochemical staining of viral nucleoprotein (brown) in lung tissue from B6 mice and D2 mice infected with 10^4 EID_{50} of HK213 virus.

tranasally inoculated B6, D2, and B6D2F1 mice with various doses of highly pathogenic H5N1 influenza A virus (HK213) and then monitored the animals' morbidity and mortality for 21 days. Inoculation with 10^6 EID_{50} resulted in 70% to 100% mortality in all three mouse strains (Fig. 1A), regardless of the age of the animal (see Table S8 in the supplemental material). In contrast, inoculation with 10^2 or 10^3 EID_{50} resulted in 80% to 100% mortality of the D2 mice, but all of the B6 and B6D2F1 mice survived. The MLD_{50} for D2 (45 EID_{50}) is significantly lower than those for B6 (6×10^5 EID_{50}, $P < 0.001$) and B6D2F1 (2×10^5 EID_{50}, $P < 0.001$).

Virus titers in lung homogenates of D2 and B6 mice were determined at various time points after inoculation with 10^4 EID_{50} of HK213 virus. Lung homogenates of D2 mice contained 10 times more infectious virus at the early postinoculation time points (24 and 48 h, $P < 0.05$) than that seen in lung homogenates of B6 mice. Four days after infection, the difference was only twofold; 7 days after infection, the difference between D2 and B6 mice was again more than 10-fold ($P < 0.05$, Fig. 1B).

Next, we quantified the amount of infectious virus present 48 h after inoculation with 10^2 or 10^3 EID_{50} of HK213 virus. At these reduced doses, infectious virus was still recovered from lung tissue of both strains of mice. Again, the virus titer was significantly higher (10-fold, $P < 0.001$) in the lungs of D2 mice (Fig. 1C). Highly pathogenic influenza viruses are known for their ability to spread systemically. Therefore, we tested for the presence of infectious virus in brain and liver tissue of these animals. None of the tissues tested contained detectable levels of infectious H5N1 virus (data not shown). Immunohistochemical analysis using a monoclonal antibody specific for the NP protein of influenza A virus confirmed the difference in viral load at 7 days postinfection (Fig. 1D).

Identification of candidate genomic loci associated with increased resistance. Phenotyping of H5N1 virus infection in B6 and D2 mice showed a clear influence of host factors on disease severity. We next applied genome-wide linkage analysis to identify the genetic element or elements responsible for survival after inoculation with H5N1 virus. We inoculated 66 different BXD RI strains with 10^4 EID_{50} of HK213 virus and then monitored the animals' survival (Fig. 2; see also Table S7 in the supplemental material and www.genenetwork.org). On average, 7.2 female mice (range, 4 to 21) were inoculated per BXD RI strain, and the majority (80%) of the strains were repeatedly tested. Because the BXD RI mice were acquired from three different sources, we compared their ages and body weights prior to infection and their mortality rates and survival times after infection. None of the tested parameters were statistically different between the BXD RI strains obtained from the Jackson Laboratory and those obtained from the ORNL,

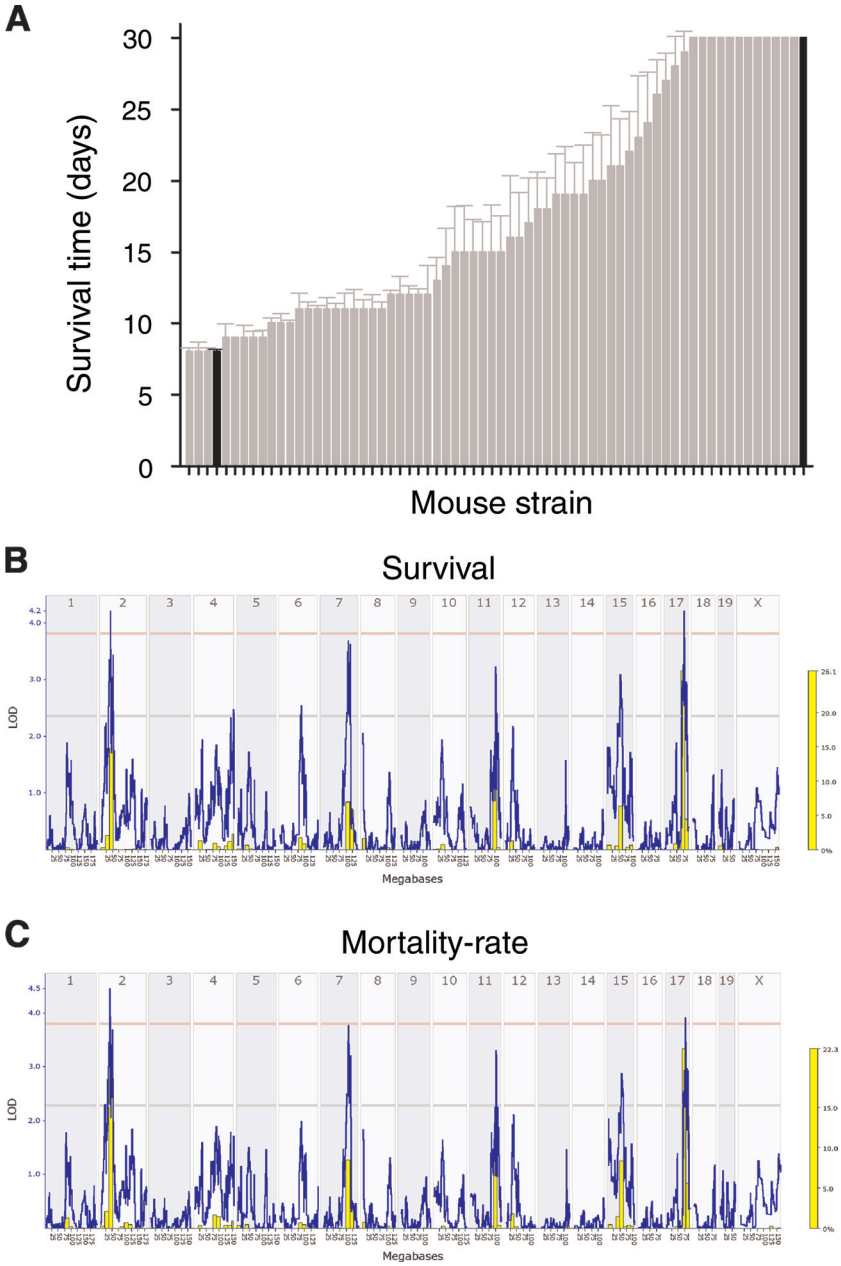

FIG. 2. Genome-wide linkage analysis for survival after H5N1 virus infection. Sixty-six different BXD RI mouse strains (derived from D2 and B6 strains) were infected with 10^4 EID_{50} of HK213 virus in 30 μl PBS. Mortality rate (measured in %) and survival (measured in days) were recorded. (A) The average survival (±standard error of the mean) is shown for each strain (gray bars) and the parental B6 and D2 strains (black bars). (B and C) QTL analysis (www.genenetwork.org) was performed on survival data (B) or mortality rate data (C). QTL associated with influenza virus resistance (*Qivr*) were located on chromosomes 2, 7, and 17, as indicated by an LOD score of more than 3.8 (pink horizontal line in QTL plot). Survival after H5N1 infection was also associated with a B6 allele on chromosome 11 and 15 with suggestive LOD scores (between pink and gray horizontal lines).

suggesting that the two sets of BXD RI strains were compatible for studying the role of host factors in disease severity following infection with H5N1 virus. The mice obtained from the University of Tennessee Health Science Center were on average 2 weeks older (data not shown) and therefore significantly larger than those obtained from the Jackson Laboratory and the ORNL (see Table S1 in the supplemental material). The increased body weight did not affect the survival time or mortality rate of these mice.

At 30 days post-inoculation with 10^4 EID_{50} of HK213 virus, the 66 BXD RI strains could be separated into three groups: group 1, containing 12 BXD RI strains, did not succumb to infection (mortality rate = 0%, survival time = 30 days) and was considered resistant to infection, similar to the parental B6

TABLE 1. Increased production of proinflammatory mediators 3 days postinfection in lungs of susceptible mice

BXD RI strain	Survival time (days)	Mortality (%)	Cytokine/chemokine production (pg/ml)			
			TNF-α	CCL2	IFN-α	IFN-β
DBA/2J	8	100	340	6,000	532	800
BXD97	9	100	86	4,371	387	—[a]
BXD67	10	100	165	3,518	250	527
BXD73	12	90	340	8,000	250	—
BXD43	30	0	53	1,834	275	370
BXD68	30	0	77	3,307	91	304
C57BL/6J	30	0	46	2,000	117	190

[a] —, not done.

mouse strains (Fig. 2A). Group 2, containing 25 BXD RI strains, was reminiscent of the D2 parental strain, i.e., the mice showed clear signs of severe disease following infection with HK213 virus and, as a result, none of the animals survived (mortality rate = 100%, survival time = 9 to 12 days). Group 3, containing 29 BXD RI strains, had an intermediate phenotype (mortality rate = 11% to 90%, survival time = 12 to 29 days).

Genome-wide linkage analysis with disease parameters, survival time, and mortality rate identified three *Qivr* on chromosomes 2 (*Qivr2*, 33 to 52 Mb), 7 (*Qivr7*, 100 to 114 Mb), and 17 (*Qivr17*, 68 to 84 Mb) that were significantly associated with resistance to infection ($P < 0.001$; Fig. 2B and C) and accounted for 7%, 5%, and 9% of the variance, respectively. Two additional *Qivr* on chromosomes 11 (*Qivr11*, 101 to 107 Mb) and 15 (*Qivr15*, 51 to 57 Mb) were not highly significant ($P < 0.05$), but their respective LOD (logarithm of the odds) scores suggest that they might be associated with resistance. *Qivr11* and *-15* accounted for 1% and 5% of the variance, respectively. Regression analysis indicated that the B6 allele had a positive effect on survival and mortality rate. To exclude the possibility of linkage disequilibrium affecting the outcome of our analysis, e.g., increasing the LOD score of unrelated peaks, we performed Spearman's rank correlation analysis on genetic loci centrally located on each of the five *Qivr*. With the exception of *Qivr15*, which was linked to both *Qivr7* and *-11* ($P < 0.05$), none of the *Qivr* were statistically linked, suggesting that each locus affects survival after a highly pathogenic H5N1 virus infection.

Increased production of proinflammatory mediators in susceptible BXD RI strains. Pathogenesis following infection with highly pathogenic H5N1 influenza A virus has been associated with increased production of cytokines and chemokines. To determine whether disease severity was correlated with inflammation in our model, we measured the production of TNF-α, IFN-α and -β, and CCL2 in D2 mice and B6 mice and in five BXD RI strains that were previously identified as either highly susceptible or resistant to infection (Table 1). Compared to the production of inflammatory mediators in uninfected D2 mice and B6 mice, that at 3 days post-infection with 10^4 EID_{50} of HK213 virus was significantly increased ($P < 0.001$; data not shown). A comparison between the strains revealed that D2 mice showed more inflammation than did B6 mice; TNF-α production was almost eightfold higher in virus-infected D2 mice than in B6 mice ($P < 0.01$), whereas IFN-α, IFN-β, and CCL2 production was approximately threefold higher ($P < 0.01$ for all three cytokines). Production of these cytokines was also determined 3 days after infection with 10^4 EID_{50} of HK213 virus in three highly susceptible (BXD67, BXD97, and BXD73) and two resistant (BXD68 and BXD43) BXD RI strains. The amount of TNF-α and CCL2 produced was higher in each of the three susceptible BXD RI strains than in the resistant BXD RI strains. Interestingly, the overall production of IFN-α and -β was higher in susceptible RI strains than in resistant RI strains, but the difference was considerably smaller, and one of the BXD RI lines (BXD43) produced amounts of IFN-α and -β that were equal to those produced by the susceptible RI lines.

Identification of candidate genes using RNA expression analysis. To identify the genes located within each of the five *Qivr* responsible for the observed differences in phenotype, we quantified RNA expression in B6 and D2 mice prior to and 3 days after infection with 10^4 EID_{50} of HK213 virus. Two-factor ANOVA identified 4,327 probes or 3,197 unique genes (reduced from 3,405 identified genes in Fig. 3A as some tran-

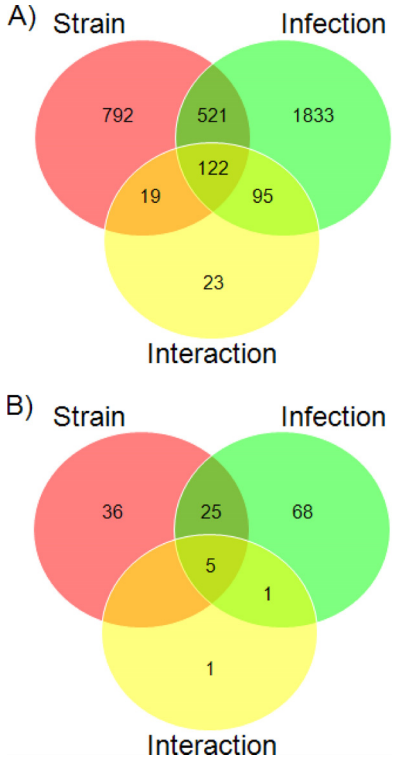

FIG. 3. RNA expression analysis in lung tissue obtained from uninfected or H5N1 virus-infected D2 mice and B6 mice. RNA expression levels were determined and analyzed. (A) Genes with an adjusted full-model *P* value of less than 0.01 (approximately 10% of the total number of probes) were selected and separated according to the three-model factor *P* values. "Strain" (red circle) indicates all genes with a significant difference (adjusted *P* value, <0.001) between DBA/2J mice and C57BL/6J mice. "Infection" (green circle) indicates all genes with a significant increase or decrease (adjusted *P* value, <0.001) in RNA expression level as a result of H5N1 virus infection. "Interaction" (yellow circle) indicates all genes with a change in RNA expression level that is dependent on the mouse strain (adjusted *P* value, <0.001). (B) All genes with an adjusted full-model *P* value of <0.01 (as shown in panel A) located within the five *Qivr* are shown.

TABLE 2. Pathway analysis with genes whose expression is significantly[a] upregulated or downregulated from baseline upon infection with H5N1 virus in D2 mice and B6 mice

Pathway	No. of genes	*P* value
Cytokine-cytokine receptor interaction	70	<0.0001
Cell adhesion molecules	46	<0.0001
Toll-like receptor signaling pathways	40	<0.0001
Type I diabetes mellitus	22	<0.0001
Antigen processing and presentation	26	<0.001
Extracellular matrix-receptor interaction	28	<0.001
Cell cycle	33	0.002
Metabolism of xenobiotics by cytochrome P450	22	0.002
P53 signaling pathway	21	0.003
Complement and coagulation cascades	22	0.006
Natural killer cell-mediated cytotoxicity	31	0.01
Urea cycle and metabolism of amino groups	11	0.02
Valine, leucine, and isoleucine degranulation	14	0.03
Glutathione metabolism	14	0.03

[a] Adjusted *P* value for infection, <0.0001 (3,179 probes).

scripts were represented in two sections of the diagram) with an adjusted full-model *P* value < 0.01 and a significant difference in one or more model factors ($P < 0.001$; Fig. 3A). Prior to infection, 792 genes were differentially expressed and reflected inherent differences in RNA expression between lungs of D2 mice and B6 mice ("Strain" [red section], Fig. 3A). Thirty-six genes were located within the *Qivr* (Fig. 3B; see also Table S2 in the supplemental material), including some that had at least a fourfold difference: *Trpc2* (transient receptor potential cation channel, subfamily C, member 2) and *Trim12* (tripartite motif-containing 12).

At 3 days post-infection with 10^4 EID_{50} of HK213 virus, the RNA expression profile was drastically altered. Of the 3,197 genes identified by the two-factor ANOVA, 1,833 were significantly up- or downregulated after infection ("Infection," $P < 0.001$ [green section]; "Strain" and "Interaction" *P* values = not significant) including 226 genes whose expression changed at least fourfold after infection in either B6 or D2 mice. Sixty-eight of the 1,833 genes were located within the *Qivr* (Fig. 3B; see also Table S3 in the supplemental material). Among those were 11 whose expression changed more than fourfold: *Trim30*, *Eif2ak2* (eukaryotic translation initiation factor 2-alpha kinase 2), and *Dhx58* (DEXH [Asp-Glu-X-His] box polypeptide 58). Clustering based on functional characteristics revealed that many of the upregulated genes were involved in cytokine-cytokine receptor signaling and Toll-like receptor signaling (Table 2); however, strain-dependent differences were observed (see Table S5 in the supplemental material).

A subset of genes (521 genes) were statistically different between B6 mice and D2 mice after infection with H5N1 virus; however, the changes in expression level following infection were similar between the two mouse strains (overlap between red and green circles, Fig. 3A). Many genes related to cytokine and chemokine signaling, as well as apoptosis, were represented in this group. A total of 25 genes were among the *Qivr*, including hemolytic complement (*Hc*), *Trim34*, interferon-induced protein 35 (*Ifi35*), and *Prkrir* (protein-kinase, interferon-inducible double-stranded RNA-dependent inhibitor, repressor of P58) (Fig. 3B; see also Table S4 in the supplemental material). In addition to the 521 genes, 122 genes were identified for which the expression varied between D2 mice and B6 mice due to infection with H5N1 virus, but the change in expression level upon infection varied significantly between the two strains ("Interaction," overlap between red, green, and yellow circles). Many of the genes, including *Ifna4*, *Tnf*, *Cxcl11*, *Cxcl2*, and *Irf1* (interferon regulatory factor 1), were associated with inflammation and antiviral immunity. Five of the 122 genes were located on a *Qivr* (Fig. 3B; see also Table S4 in the supplemental material) and included a *Trim30*-like gene (*AI451617*), *Plekhb1* (pleckstrin homology domain-containing, family B [evectins] member 1), *Ifi35*, granulin (*Grn*), and *Cox7a2l*. Finally, 95 genes were identified with significant *P* values for "Infection" and "Interaction," but their expression level was not significantly different between the two strains (overlap between yellow and green circles, Fig. 3A). Only one gene, xanthine dehydrogenase (*Xdh*), was located on a *Qivr* (Fig. 3B). To summarize, RNA expression analysis identified 121 unique candidate genes (reduced from 136 as shown in Fig. 3B, as some genes were represented in more than one section of the diagram) whose genetic polymorphisms or differences in expression level can have a significant effect on H5N1 pathogenesis.

Expression profiling in H5N1 virus-infected BXD RI lines. RNA expression profiling was performed on several BXD RI lines infected with HK213 virus for 72 h. The four susceptible BXD lines (-67, -73, -83, and -97) had an average survival time of 10.5 days, and all mice succumbed to infection. Resistant BXD RI lines (-43, -68, and -98) had an average survival time of 29.3 days, and their mortality rate was less than 2%. Comparison of RNA expression between resistant and susceptible mice, including the parental D2 and B6 strains, identified many genes whose expression differed significantly (>2-fold, $P < 0.01$). These genes included several immune response-related genes like *Ifn*-β and *CCL5* (see Table S6 in the supplemental material). Of the 121 *Qivr* genes previously identified by our full-model analysis using B6 mice and D2 mice, 30 candidate genes were also differentially expressed ($P < 0.001$) between the susceptible and resistant BXD RI strains (Table 3). *Qivr2* has three candidate genes: *Hc*, gelsolin (*Gsn*), and a sialidase transferase gene (*St6galnac4*). The largest locus, *Qivr7*, has 14 candidate genes including *Trim12* and *Trim34*, as well as several other interesting gene candidates such as *Plekhb1*, *Prkrir*, and *Trpc2*. *Qivr11* contained five genes whose expression differed significantly between the susceptible and resistant mouse strains: *Grn*, *Ifi35*, *Med1*, *Pitpnc1*, and *Ubtf*. Only two candidate genes on *Qivr15* were identified by this analysis, *Nov* and *Depdc6*. Finally, for *Qivr17*, six candidate genes were identified, including *Prkcn*, *Qpct*, *Dlgap1*, and *Mta3*, whose polymorphisms or expression levels may alter the outcome after infection with H5N1 viruses.

Effect of hemolytic complement on survival following H5N1 virus infection. To partially validate our approach for identifying functionally relevant host genes, we chose one gene for further analysis, *Hc*, whose expression segregated with disease severity and was located on *Qivr2*. D2 mice, as well as many other inbred strains, do not produce mature, functional *Hc* protein (30, 34). *Hc* deficiency was previously reported to increase susceptibility to other infectious agents, including mouse-adapted influenza A virus (20, 43). To study the effect of *Hc* on survival after inoculation with a highly pathogenic H5N1

TABLE 3. *Qivr* candidate genes based on RNA expression differences between susceptible and resistant mice[a]

Qivr	Gene symbol	Gene name	Probe identifier
2	*Gsn*	Gelsolin	1415812_at
	Hc	Hemolytic complement	1419407_at
	St6galnac4	GalNAc-alpha-2,6-sialyltransferase	1418074_at
7	*A530023O14Rik*	Hypothetical protein	1444179_at
	EG667823	Hypothetical protein	1442693_at
	Fam168a	Hypothetical protein	1434375_at
	Myo7a	Myosin VIIA	1421385_a_at
	Phca	Phytoceramidase, alkaline	1438435_at
	Plekhb1	Pleckstrin homology domain-containing, family B (evectins) member 1	1416178_a_at
	Prkrir	Protein kinase, interferon-inducible double-stranded RNA-dependent inhibitor, repressor of (P58 repressor)	1426482_at
	Rassf10	Ras association (RalGDS/AF-6) domain family (N-terminal) member 10	1457140_s_at
	Rnf121	Ring finger protein 121	1426504_a_at
	Rps3	Ribosomal protein 3	1455600_at
	Slco2b1	Solute carrier organic anion transporter family, member 2b1	1433933_s_at
	Trim12	Tripartite motif-containing 12	1437432_a_at
	Trim34	Tripartite motif-containing 34	1424857_a_at
	Trpc2	Transient receptor potential cation channel, subfamily C, member 2	1430485_at
11	*Grn*	Granulin (proepithelin)	1448148_at
	Ifi35	Interferon-induced protein 35	1424617_at/1459151_x_at
	Med1	Mediator complex subunit 1	1448708_at
	Pitpnc1	Phosphatidylinositol transfer protein, cytoplasmic 1	1428879_at
	Ubtf	Upstream binding transcription factor, RNA polymerase I	1455490_at
15	*Depdc6*	DEP domain-containing 6	1453571_at
	Nov	Nephroblastoma overexpressed gene	1426852_x_at/1426851_a_at
17	*2410091C18Rik*	Hypothetical protein	1427904_s_at
	Cdc42ep3	CDC42 effector protein (Rho GTPase binding) 3	1450700_at
	Dlgap1	Discs, large (*Drosophila*) homolog-associated protein 1	1436076_at
	Mta3	Metastasis-associated 1 family, member 3	1421402_at
	Prkcn	Protein kinase D3	
	Qpct	Glutaminyl-peptide cyclotransferase (glutaminyl cyclase)	1426622_a_at

[a] RNA expression was compared between susceptible (D2 and BXD67, -73, -83, and -97) and resistant (B6 and BXD43, -68, and -98) strains of mice after infection with H5N1 virus.

virus, we infected two mouse strains, one that expressed *Hc* (B10.D2.Hc^1) and one that did not (B10.D2.Hc^0). Inoculation of B10.D2.Hc^0 mice with 10^4 EID_{50} of HK213 virus resulted in 74% mortality, while all of the B10.D2.Hc^1 mice survived (Fig. 4A; $P < 0.001$). Increased survival of *Hc*-positive mice was also observed at a 10-fold-higher initial inoculum (10^5 EID_{50}), supporting the role of *Qivr2* in resistance to H5N1 infection. Several members of the complement cascade have been shown to influence the adaptive immune response to infectious agents including viruses (25, 29). Efficient immune responses are associated with the clearance of the virus, and low viral loads at later stages of the infection are indicative of this. At 7 days post-infection with 10^4 EID_{50} of HK213 virus, the viral load in the lungs of the B10.D2.Hc^0 mice was significantly higher than that in the lungs of the B10.D2.Hc^1 mice (Fig. 4B; $P < 0.05$), while the viral load on day 4 was similar. These data suggest that *Hc* significantly affects the outcome of infection with highly pathogenic H5N1 virus.

DISCUSSION

The current study was designed to assess the effect of genetic variation in the host on survival after infection with a highly pathogenic H5N1 influenza virus. Applying the murine model of H5N1 influenza virus infection, we showed that genetic variation significantly contributes to survival. QTL mapping identified five loci associated with severity of disease after H5N1 virus infection, indicating that multiple genes are responsible for the observed difference. RNA expression analysis has resulted in several candidate genes whose function is potentially linked to infection or inflammation.

Following the initial observation that certain mouse strains are more susceptible to severe disease after infection with highly pathogenic avian H5N1 influenza A virus but that other strains are resistant to disease, we sought to identify the underlying mechanism responsible for this difference. Susceptible mice that succumbed after infection had high viral loads and increased production of proinflammatory cytokines early after infection. In contrast, resistant mice that effectively cleared the infection had reduced virus titers and produced lower levels of proinflammatory cytokines. This link between disease severity and high viral loads plus increased production of proinflammatory cytokines was previously found in humans infected with H5N1 viruses (12). de Jong et al. (12) observed in a cohort of H5N1 virus-infected individuals that high viral loads in throat swabs and the presence of high concentrations of TNF-α and CCL2 in serum were associated with poor prognosis. In studies comparing pathogenicities of different influenza A virus

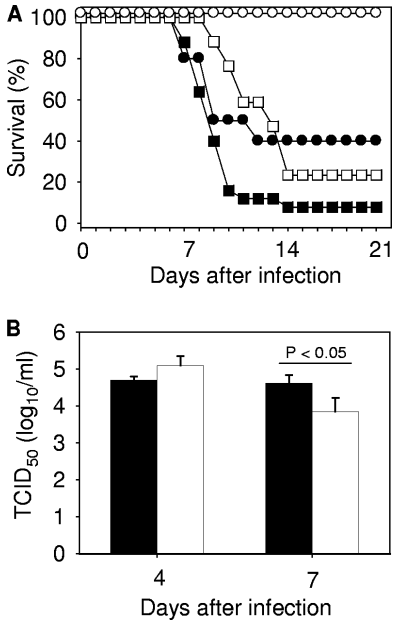

FIG. 4. Effect of hemolytic complement on mortality after infection with highly pathogenic H5N1 influenza A virus. (A) Hemolytic complement (*Hc*)-deficient mice (B10.D2.Hc^0, solid symbols) and *Hc*-sufficient mice (B10.D2.Hc^1, open symbols) were infected with 10^4 EID_{50} (circles) or 10^5 EID_{50} (squares) of a highly pathogenic H5N1 influenza A virus (A/Hong Kong/213/03 [HK213]), and survival was determined for 21 days postinfection. (B) At 4 and 7 days post-infection with 10^4 EID_{50} of HK213 virus, lungs were isolated from B10.D2.Hc^0 mice and B10.D2.Hc^1 mice. The viral load on day 7 in the *Hc*-deficient lungs was significantly higher than that in the *Hc*-sufficient lungs. $TCID_{50}$, 50% tissue culture infective dose.

strains, high viral load combined with increased levels of proinflammatory cytokines was also associated with severe disease and increased mortality (22–24).

An important and novel finding of this study is that H5N1-induced pathology is greatly affected by genetic polymorphisms in the genome of the infected host. We have also found that, at least in mice, H5N1 pathogenesis is a complex genetic trait with multiple genes affecting disease outcome. This result is reminiscent of many other microbial diseases including human immunodeficiency virus infection and *Mycobacterium tuberculosis* infection (3, 7, 8, 15, 17, 47). A possible explanation for the observed complexity is the nature of the pathogen, e.g., viral, requiring a host cell for propagation. Following attachment, fusion, replication, and assembly of progeny virus in the host cell, an innate and adaptive immune response is initiated to eliminate the pathogen in a time- and energy-efficient manner. The many genes involved in this process can all greatly influence the outcome of the disease. Our approach of combining QTL mapping with RNA expression analysis at day 3 has shifted the focus to identifying genes involved in viral replication or early innate immune responses. However, the identification of *Hc*, the candidate gene on *Qivr2*, is an example of a protein involved and required for effective adaptive immune responses.

The highly pathogenic A/Hong Kong/213/03 influenza A virus was used to identify host genes and gene networks promoting survival after infection. It was selected from several H5N1 viruses for its extremely large difference in LD_{50} (>10,000-fold) between the two parental mouse strains B6 and D2. Other H5N1 viruses, including A/Vietnam/1203/04 virus, demonstrated increased lethality to B6 mice, effectively reducing our difference in LD_{50} and potentially compromising our genetic screen. Preliminary studies were also done with the mouse-adapted A/Puerto Rico/8/34 virus (PR8) (data not shown). For this particular virus, the difference in LD_{50} between D2 and B6 mice is approximately 100-fold (data not shown) (32). Also, we measured survival in 13 BXD RI strains after infection with an intermediate dose of PR8. BXD strains with severe PR8-induced pathology were also among the most susceptible to HK213 virus, suggesting that some of the candidate genes identified in this study are important for survival after influenza virus infection in general. The identification of *Hc* supports this, as it was first shown to be important for survival after infection with A/PR/8/34 influenza A virus.

It is tempting to speculate that certain genetic deficiencies identified in this study are universally associated with increased susceptibility to influenza virus and potentially other viruses like Sendai virus. An example of this is *Hc*, which was shown to affect survival after inoculation with a highly pathogenic H5N1 influenza virus, supporting a previous publication demonstrating a similar effect of *Hc* after inoculation with PR8 or X31 (an H3N2 virus with the internal genes of PR8). Our study, however, is also likely to identify genes whose deficiency affects specifically H5N1 influenza A virus-induced disease because of the difference in pathology between highly pathogenic and low-pathogenic influenza A viruses (4).

To identify candidate genes within each of the five *Qivr*, we analyzed the pattern of RNA expression. This methodology has been effective in the past and allows for the identification of genes responsible for infectious diseases or immune system-related phenotypes (16, 27). One of the three candidate genes on *Qivr2*, *Hc*, was previously shown to be involved in both the innate and adaptive immune responses to infectious agents including low-pathogenic mouse-adapted influenza viruses (20). We have now shown that *Hc* is also important for adequate adaptive immune responses to H5N1 viruses, as indicated by the higher viral loads in *Hc*-deficient mice (Fig. 1B and 4B). Although this is not surprising, considering the previously identified role for *Hc* in the inflammatory response to low-pathogenic viruses, the confirmation illustrates the usefulness of RNA expression analysis to identify the gene within a QTL responsible for the increased resistance to infection.

The identity of the underlying genetic variation in the other three loci (*Qivr7*, *-11*, and *-17*) is currently unknown; however, we have identified several candidate genes based on expression levels, the presence of a single nucleotide polymorphism encoding an amino acid change, and previously published literature. The main candidates for *Qivr7* are *Trim12*, *Trim34*, *Trim30*-like (*AI451617*), and *Gvin1* (very large interferon-inducible GTPase). *Trim30* limits the response of macrophages to Toll-like receptor stimuli through binding to TBK1 (40); other Trim proteins were shown to have antiviral properties (10, 31, 45, 48). Several Trim genes, including *Trim30* and *Trim34*, were upregulated in macrophages and dendritic cells maintained in culture upon exposure to influenza A virus (H1N1) (37). For *Qivr11*, we identified three potential candidate genes: *Grn*, *Ifi35*, and *Dhx58*. *Ifi35* is induced upon expo-

sure to interferon and is reported to modulate cytokine signaling (49). *Ifi35* also has antiviral properties against bovine foamy virus (41). *Qivr17* contains several candidate genes including *Eif2ak2* and *Xdh*, two genes with known roles in influenza virus infection (1, 5). However, neither protein contains any single nucleotide polymorphism encoding an amino acid change. Other candidate genes on *Qivr17* are *Emilin2* (elastin microfibril interfacer 2), encoding a protein that has affinity for the protective antigen of the anthrax bacterium and is involved in the extrinsic apoptosis pathway (14, 28), and *Ipaf*, an intracellular pattern-recognition receptor (18).

A more detailed analysis of expression levels and identification of important gene networks differentially expressed following infection enable further selection of genes among the relatively large number of candidate genes. A significant drawback of this approach is that the gene of interest must demonstrate a difference in expression level, certainly not a prerequisite for differential activity, and that the gene of interest or a splice variant must be detected by the microchip. When genetic changes affect function but not expression level, downstream effects of this particular change can then be used to identify the gene of interest. Overall, this technique, despite its limitations, is considered an important tool for selecting candidate genes within a QTL and one which we have used here.

Collectively, our results show that host genetic variation has a significant impact on survival after infection with a highly pathogenic H5N1 influenza A virus, which is associated with lower viral loads and reduced levels of proinflammatory cytokines, both of which are hallmarks of a mild H5N1 virus infection in humans. Gene mapping and RNA expression analysis have identified several candidate genes, whose genetic variation may ultimately determine the outcome after infection. Our study has convincingly shown a dramatic effect of host genetics on H5N1 virus infection, supporting those studies claiming a genetic predisposition in humans. This study provides a list of priority genes which should be closely examined in family clusters of H5N1 virus infection in humans.

ACKNOWLEDGMENTS

We thank Kelli Boyd and Dorothy Bush for performing and analyzing influenza A virus immunohistochemistry. We also acknowledge Robert Webster and Mariette Ducatez for critically reviewing the manuscript and M. Sandbulte for helpful discussions. We thank D. Carey and S. Krauss for their help in the ABSL3+ facility.

REFERENCES

1. **Akaike, T., M. Ando, T. Oda, T. Doi, S. Ijiri, S. Araki, and H. Maeda.** 1990. Dependence on O2− generation by xanthine oxidase of pathogenesis of influenza virus infection in mice. J. Clin. Investig. **85:**739–745.
2. **Albright, F. S., P. Orlando, A. T. Pavia, G. G. Jackson, and L. A. C. Albright.** 2008. Evidence for a heritable predisposition to death due to influenza. J. Infect. Dis. **197:**18–24.
3. **Alcais, A., M. Mira, J. L. Casanova, E. Schurr, and L. Abel.** 2005. Genetic dissection of immunity in leprosy. Curr. Opin. Immunol. **17:**44–48.
4. **Aldridge, J. R., Jr., C. E. Moseley, D. A. Boltz, N. J. Negovetich, C. Reynolds, J. Franks, S. A. Brown, P. C. Doherty, R. G. Webster, and P. G. Thomas.** 2009. TNF/iNOS-producing dendritic cells are the necessary evil of lethal influenza virus infection. Proc. Natl. Acad. Sci. USA **106:**5306–5311.
5. **Balachandran, S., P. C. Roberts, L. E. Brown, H. Truong, A. K. Pattnaik, D. R. Archer, and G. N. Barber.** 2000. Essential role for the dsRNA-dependent protein kinase PKR in innate immunity to viral infection. Immunity **13:**129–141.
6. **Benjamini, Y., and Y. Hochberg.** 1995. Controlling the false discovery rate: a practical and powerful approach to multiple testing. J. R. Stat. Soc. Ser. B **57:**289–300.
7. **Beutler, B., K. Crozat, J. A. Koziol, and P. Georgel.** 2005. Genetic dissection of innate immunity to infection: the mouse cytomegalovirus model. Curr. Opin. Immunol. **17:**36–43.
8. **Beutler, B., C. Eidenschenk, K. Crozat, J. L. Imler, O. Takeuchi, J. A. Hoffmann, and S. Akira.** 2007. Genetic analysis of resistance to viral infection. Nat. Rev. Immunol. **7:**753–766.
9. **Boon, A. C. M., G. de Mutsert, Y. M. F. Graus, R. A. M. Fouchier, K. Sintnicolaas, A. D. M. E. Osterhaus, and G. F. Rimmelzwaan.** 2002. The magnitude and specificity of influenza A virus-specific cytotoxic T-lymphocyte responses in humans is related to HLA-A and -B phenotype. J. Virol. **76:**582–590.
10. **Chelbi-Alix, M. K., F. Quignon, L. Pelicano, M. H. M. Koken, and H. de Thé.** 1998. Resistance to virus infection conferred by the interferon-induced promyelocytic leukemia protein. J. Virol. **72:**1043–1051.
11. **Chesler, E. J., L. Lu, S. Shou, Y. Qu, J. Gu, J. Wang, H. C. Hsu, J. D. Mountz, N. E. Baldwin, M. A. Langston, D. W. Threadgill, K. F. Manly, and R. W. Williams.** 2005. Complex trait analysis of gene expression uncovers polygenic and pleiotropic networks that modulate nervous system function. Nat. Genet. **37:**233–242.
12. **de Jong, M. D., C. P. Simmons, T. T. Thanh, V. M. Hien, G. J. Smith, T. N. Chau, D. M. Hoang, N. V. Chau, T. H. Khanh, V. C. Dong, P. T. Qui, B. V. Cam, D. Q. Ha, Y. Guan, J. S. Peiris, N. T. Chinh, T. T. Hien, and J. Farrar.** 2006. Fatal outcome of human influenza A (H5N1) is associated with high viral load and hypercytokinemia. Nat. Med. **12:**1203–1207.
13. **Dittmann, J., S. Stertz, D. Grimm, J. Steel, A. Garcia-Sastre, O. Haller, and G. Kochs.** 2008. Influenza A virus strains differ in sensitivity to the antiviral action of Mx-GTPase. J. Virol. **82:**3624–3631.
14. **Doliana, R., V. Veljkovic, J. Prljic, N. Veljkovic, E. De Lorenzo, M. Mongiat, G. Ligresti, S. Marastoni, and A. Colombatti.** 2008. EMILINs interact with anthrax protective antigen and inhibit toxin action in vitro. Matrix Biol. **27:**96–106.
15. **Fellay, J., K. V. Shianna, D. Ge, S. Colombo, B. Ledergerber, M. Weale, K. Zhang, C. Gumbs, A. Castagna, A. Cossarizza, A. Cozzi-Lepri, A. De Luca, P. Easterbrook, P. Francioli, S. Mallal, J. Martinez-Picado, J. M. Miro, N. Obel, J. P. Smith, J. Wyniger, P. Descombes, S. E. Antonarakis, N. L. Letvin, A. J. McMichael, B. F. Haynes, A. Telenti, and D. B. Goldstein.** 2007. A whole-genome association study of major determinants for host control of HIV-1. Science **317:**944–947.
16. **Fisher, P., C. Hedeler, K. Wolstencroft, H. Hulme, H. Noyes, S. Kemp, R. Stevens, and A. Brass.** 2007. A systematic strategy for large-scale analysis of genotype phenotype correlations: identification of candidate genes involved in African trypanosomiasis. Nucleic Acids Res. **35:**5625–5633.
17. **Fortin, A., L. Abel, J. L. Casanova, and P. Gros.** 2007. Host genetics of mycobacterial diseases in mice and men: forward genetic studies of BCG-osis and tuberculosis. Annu. Rev. Genomics Hum. Genet. **8:**163–192.
18. **Fritz, J. H., R. L. Ferrero, D. J. Philpott, and S. E. Girardin.** 2006. Nod-like proteins in immunity, inflammation and disease. Nat. Immunol. **7:**1250–1257.
19. **Gottfredsson, M., B. V. Halldorsson, S. Jonsson, M. Kristjansson, K. Kristjansson, K. G. Kristinsson, A. Love, T. Blondal, C. Viboud, S. Thorvaldsson, A. Helgason, J. R. Gulcher, K. Stefansson, and I. Jonsdottir.** 2008. Lessons from the past: familial aggregation analysis of fatal pandemic influenza (Spanish flu) in Iceland in 1918. Proc. Natl. Acad. Sci. USA **105:**1303–1308.
20. **Hicks, J. T., F. A. Ennis, E. Kim, and M. Verbonitz.** 1978. The importance of an intact complement pathway in recovery from a primary viral infection: influenza in decomplemented and in C5-deficient mice. J. Immunol. **121:**1437–1445.
21. **Hoffmann, E., G. Neumann, Y. Kawaoka, G. Hobom, and R. G. Webster.** 2000. A DNA transfection system for generation of influenza A virus from eight plasmids. Proc. Natl. Acad. Sci. USA **97:**6108–6113.
22. **Kash, J. C., T. M. Tumpey, S. C. Proll, V. Carter, O. Perwitasari, M. J. Thomas, C. F. Basler, P. Palese, J. K. Taubenberger, A. Garcia-Sastre, D. E. Swayne, and M. G. Katze.** 2006. Genomic analysis of increased host immune and cell death responses induced by 1918 influenza virus. Nature **443:**578–581.
23. **Kobasa, D., S. M. Jones, K. Shinya, J. C. Kash, J. Copps, H. Ebihara, Y. Hatta, J. H. Kim, P. Halfmann, M. Hatta, F. Feldmann, J. B. Alimonti, L. Fernando, Y. Li, M. G. Katze, H. Feldmann, and Y. Kawaoka.** 2007. Aberrant innate immune response in lethal infection of macaques with the 1918 influenza virus. Nature **445:**319–323.
24. **Kobasa, D., A. Takada, K. Shinya, M. Hatta, P. Halfmann, S. Theriault, H. Suzuki, H. Nishimura, K. Mitamura, N. Sugaya, T. Usui, T. Murata, Y. Maeda, S. Watanabe, M. Suresh, T. Suzuki, Y. Suzuki, H. Feldmann, and Y. Kawaoka.** 2004. Enhanced virulence of influenza A viruses with the haemagglutinin of the 1918 pandemic virus. Nature **431:**703–707.
25. **Kopf, M., B. Abel, A. Gallimore, M. Carroll, and M. F. Bachmann.** 2002. Complement component C3 promotes T-cell priming and lung migration to control acute influenza virus infection. Nat. Med. **8:**373–378.
26. **Liu, R., W. A. Paxton, S. Choe, D. Ceradini, S. R. Martin, R. Horuk, M. E. MacDonald, H. Stuhlmann, R. A. Koup, and N. R. Landau.** 1996. Homozygous defect in HIV-1 coreceptor accounts for resistance of some multiply-exposed individuals to HIV-1 infection. Cell **86:**367–377.
27. **Miyairi, I., V. R. Tatireddigari, O. S. Mahdi, L. A. Rose, R. J. Belland, L. Lu,**

R. W. Williams, and G. I. Byrne. 2007. The p47 GTPases Iigp2 and Irgb10 regulate innate immunity and inflammation to murine Chlamydia psittaci infection. J. Immunol. **179:**1814–1824.
28. **Mongiat, M., G. Ligresti, S. Marastoni, E. Lorenzon, R. Doliana, and A. Colombatti.** 2007. Regulation of the extrinsic apoptotic pathway by the extracellular matrix glycoprotein EMILIN2. Mol. Cell. Biol. **27:**7176–7187.
29. **Moulton, R. A., M. A. Mashruwala, A. K. Smith, D. R. Lindsey, R. A. Wetsel, D. L. Haviland, R. L. Hunter, and C. Jagannath.** 2007. Complement C5a anaphylatoxin is an innate determinant of dendritic cell-induced Th1 immunity to Mycobacterium bovis BCG infection in mice. J. Leukoc. Biol. **82:**956–967.
30. **Nilsson, U. R., and H. J. Muller-Eberhard.** 1967. Deficiency of the fifth component of complement in mice with an inherited complement defect. J. Exp. Med. **125:**1–16.
31. **Nisole, S., J. P. Stoye, and A. Saib.** 2005. TRIM family proteins: retroviral restriction and antiviral defence. Nat. Rev. Microbiol. **3:**799–808.
32. **Nohara, K., H. Izumi, S. Tamura, R. Nagata, and C. Tohyama.** 2002. Effect of low-dose 2,3,7,8-tetrachlorodibenzo-p-dioxin (TCDD) on influenza A virus-induced mortality in mice. Toxicology **170:**131–138.
33. **Olsen, S. J., K. Ungchusak, L. Sovann, T. M. Uyeki, S. F. Dowell, N. J. Cox, W. Aldis, and S. Chunsuttiwat.** 2005. Family clustering of avian influenza A (H5N1). Emerg. Infect. Dis. **11:**1799–1801.
34. **Ooi, Y. M., and H. R. Colten.** 1979. Genetic defect in secretion of complement C5 in mice. Nature **282:**207–208.
35. **Peirce, J. L., L. Lu, J. Gu, L. M. Silver, and R. W. Williams.** 2004. A new set of BXD recombinant inbred lines from advanced intercross populations in mice. BMC Genet. **5:**7.
36. **Pitzer, V. E., S. J. Olsen, C. T. Bergstrom, S. F. Dowell, and M. Lipsitch.** 2007. Little evidence for genetic susceptibility to influenza A (H5N1) from family clustering data. Emerg. Infect. Dis. **13:**1074–1076.
37. **Rajsbaum, R., J. P. Stoye, and A. O'Garra.** 2008. Type I interferon-dependent and -independent expression of tripartite motif proteins in immune cells. Eur. J. Immunol. **38:**619–630.
38. **Reed, L. J., and H. Muench.** 1938. A simple method for estimating fifty percent endpoints. Am. J. Hyg. **27:**493–497.
39. **Salomon, R., P. Staeheli, G. Kochs, H. L. Yen, J. Franks, J. E. Rehg, R. G. Webster, and E. Hoffmann.** 2007. Mx1 gene protects mice against the highly lethal human H5N1 influenza virus. Cell Cycle **6:**2417–2421.
40. **Shi, M., W. Deng, E. Bi, K. Mao, Y. Ji, G. Lin, X. Wu, Z. Tao, Z. Li, X. Cai, S. Sun, C. Xiang, and B. Sun.** 2008. TRIM30 alpha negatively regulates TLR-mediated NF-kappa B activation by targeting TAB2 and TAB3 for degradation. Nat. Immunol. **9:**369–377.
41. **Tan, J., W. Qiao, J. Wang, F. Xu, Y. Li, J. Zhou, Q. Chen, and Y. Geng.** 2008. IFP35 is involved in the antiviral function of interferon by association with the viral Tas transactivator of bovine foamy virus. J. Virol. **82:**4275–4283.
42. **Taylor, B. A., C. Wnek, B. S. Kotlus, N. Roemer, T. MacTaggart, and S. J. Phillips.** 1999. Genotyping new BXD recombinant inbred mouse strains and comparison of BXD and consensus maps. Mamm. Genome **10:**335–348.
43. **Tuite, A., M. Elias, S. Picard, A. Mullick, and P. Gros.** 2005. Genetic control of susceptibility to Candida albicans in susceptible A/J. and resistant C57BL/6J mice. Genes Immun. **6:**672–682.
44. **Tumpey, T. M., K. J. Szretter, N. Van Hoeven, J. M. Katz, G. Kochs, O. Haller, A. Garcia-Sastre, and P. Staeheli.** 2007. The *Mx1* gene protects mice against the pandemic 1918 and highly lethal human H5N1 influenza viruses. J. Virol. **81:**10818–10821.
45. **Uchil, P. D., B. D. Quinlan, W. T. Chan, J. M. Luna, and W. Mothes.** 2008. TRIM E3 ligases interfere with early and late stages of the retroviral life cycle. PLoS Pathog. **4:**e16.
46. **Vanlaere, I., A. Vanderrijst, J. L. Guenet, M. De Filette, and C. Libert.** 2008. Mx1 causes resistance against influenza A viruses in the Mus spretus-derived inbred mouse strain SPRET/Ei. Cytokine **42:**62–70.
47. **Vidal, S. M., D. Malo, J. F. Marquis, and P. Gros.** 2008. Forward genetic dissection of immunity to infection in the mouse. Annu. Rev. Immunol. **26:**81–132.
48. **Wolf, D., and S. P. Goff.** 2007. TRIM28 mediates primer binding site-targeted silencing of murine leukemia virus in embryonic cells. Cell **131:**46–57.
49. **Zhang, L., Y. Tang, Y. Tie, C. Tian, J. Wang, Y. Dong, Z. Sun, and F. He.** 2007. The PH domain containing protein CKIP-1 binds to IFP35 and Nmi and is involved in cytokine signaling. Cell. Signal. **19:**932–944.
50. **Zhang, S. Y., E. Jouanguy, S. Ugolini, A. Smahi, G. Elain, P. Romero, D. Segal, V. Sancho-Shimizu, L. Lorenzo, A. Puel, C. Picard, A. Chapgier, S. Plancoulaine, M. Titeux, C. Cognet, H. von Bernuth, C. L. Ku, A. Casrouge, X. X. Zhang, L. Barreiro, J. Leonard, C. Hamilton, P. Lebon, B. Heron, L. Vallee, L. Quintana-Murci, A. Hovnanian, F. Rozenberg, E. Vivier, F. Geissmann, M. Tardieu, L. Abel, and J. L. Casanova.** 2007. TLR3 deficiency in patients with herpes simplex encephalitis. Science **317:**1522–1527.